

Cryomechanical freezing. A model for the heat transfer process

Miriam E. Agnelli^{a,b}, Rodolfo H. Mascheroni^{a,b,*}

^a Centro de Investigación y Desarrollo en Criotecnología de Alimentos (UNLP-CONICET), Universidad Nacional de la Plata,
47 y 116 (1900), La Plata, Argentina

^b MODIAL, Facultad de Ingeniería, UNLP, La Plata, Argentina

Received 10 March 2000; accepted 24 July 2000

Abstract

Cryomechanical freezing consists of a two-step process. During the first step, the foodstuff gets into contact with a cryogenic refrigerant for a very short period of time, during which a thin frozen crust is formed. Immediately afterwards, freezing is completed in a conventional cold air-blast freezer. In this work, the heat transfer process during cryomechanical freezing was modelled using the enthalpy formulation with a finite volume scheme. The results of the model were successfully compared with experimental data obtained in the literature for a model food (cylinders of gelatin) and for real foodstuffs (hamburgers, meatballs and strawberries) in a pilot prototype. © 2000 Elsevier Science Ltd. All rights reserved.

Keywords: Cryogenic; Freezing; Crust; Model

1. Introduction

Cryomechanical freezing consists of the association of two freezing systems: an on-line cryogenic immersion freezer (using a cryogenic fluid like liquid N₂ or CO₂) combined with a mechanical freezer (with cold air produced by a conventional refrigeration equipment). The combined process uses the following sequence for most cases (Groll, 1986; Acharya, Marchese, & Bredencamp, 1989):

(1) *Cryogenic freezing*. When the foodstuff is submerged in the cryogenic liquid, a fast freezing of the outer layers occurs forming a thin crust. This freeze-crusting treatment provides a higher resistance strength to the foodstuff and prevents small and/or wet products from sticking on the conveyor or between them.

(2) *Mechanical freezing*. The freeze-crusting product completes its freezing until the centre of the foodstuff reaches the required final temperature.

The use of the combined freezer provokes a reduction of the freezing time and of water loss during the process. These reductions may cause an improvement in the final quality of the product (Summers, 1986; Londahl & Goranson, 1995). Besides, the combined system also offers a simple and economical solution to increase freezing capacity (Gruda, 1999). However, its most im-

portant application is for freezing of delicate products, i.e., products not having a good mechanical resistance (strawberries, raspberries, shrimps) or products that otherwise change their appearance (chicken scallops). Another important use is for food pieces that tend to stick or clump (diced potatoes). In these cases, the higher cost caused by liquid nitrogen (LN) consumption, is compensated by the attainment of a product with a lower weight loss and a higher final quality or an overall better appearance.

The key to make cryomechanical freezing profitable is to provide the minimum viable product crust thickness to avoid undue consumption of LN. The general objective is to enable the product to be crusted in the shortest time of immersion in LN. A theoretical model of the combined process constitutes a valuable support for this purpose. Thus, the necessary time for each step (immersion and freezing completion) for reaching the desired conditions can be predicted in advance.

In the present work, we propose a model for the combined freezing process that is then developed to a numerical prediction algorithm. The results of this model are first compared with experimental data taken from the literature for a model food (cylinders of gelatin, Macchi (1995)). Then, the model is tested for real foods with data obtained in our laboratory prototype. Quality aspects related to the application of cryomechanical freezing will be treated in a further work.

* Corresponding author. Fax: +54-221-424-9287.

E-mail address: rhmasche@volta.ing.unlp.edu.ar (R.H. Mascheroni).

Notation			
C_p	heat capacity ($\text{J kg}^{-1} \text{ } ^\circ\text{C}^{-1}$)	S	surface area (m^2)
h	heat transfer coefficient ($\text{W m}^{-2} \text{ K}^{-1}$)	t	time (s)
H	enthalpy (J kg^{-1})	T	temperature ($^\circ\text{C}$)
i	space index	T_f	initial phase change temperature
k	thermal conductivity ($\text{W m}^{-1} \text{ } ^\circ\text{C}^{-1}$)	T_∞	ambient temperature ($^\circ\text{C}$)
m	mass (kg)	V	volume (m^3)
r	radius (m)	Y_o	water content
		ρ	density (kg m^{-3})

2. Experimental

Product freezing. Hamburgers, meatballs and strawberries were frozen following the same procedure: products were submerged for a given time in LN (a few seconds) and then placed in the air-blast freezer till the core temperature reached -20°C . The characteristics of each product and the conditions for their freezing are given in Table 1.

In each freezing test, the core temperature evolution in time was followed by means of a type T thermocouple connected to a data acquisition system Keithley DAC 500.

Measurement of heat transfer coefficients. Heat transfer coefficients for cryogenic and mechanical steps were experimentally determined from the thermal histories of bodies constructed in aluminum with shapes and dimensions similar to the treated foodstuffs. For hamburgers, a disk in the sizes indicated in Table 1 was made and pierced at mid-height along a radius in order to place a thermocouple in the centre of the body. For meatballs and strawberries, the procedure was identical but using a sphere and a combined geometrical figure composed by a cone and hemisphere respectively, both with similar dimensions to those of the products (Table 1). The value of the heat transfer coefficient h was calculated solving the heat transfer balance assuming a constant temperature in the interior of the body. This is true due to the high thermal conductivity for aluminum. Thus, the thermal flux of the aluminum body submerged in a cool fluid (LN or cold air) is given by:

$$mC_p \frac{dT}{dt} = hA(T_\infty - T),$$

where m is the mass of the body, A its surface area, C_p its heat capacity, T the temperature, T_∞ the external temperature (constant) and t is the time.

Integrating, we obtain

$$\ln T^* = \ln \frac{(T_\infty - T)}{(T_\infty - T_0)} = -\frac{hA}{mC_p} t.$$

So, plotting $\ln T^*$ vs t , we can obtain the value of h from the slope.

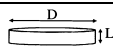
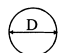

Crust thickness measurement. The thickness of the crust was measured on strawberries from photographs and image analysis of halved samples. A photograph of the crust-frozen strawberry in LN was taken after the crust had thawed. The boundary between the frozen and unfrozen zones could be easily distinguished by simple visual inspection. However, it was not clear enough for an image analyzer. So, photographs were enhanced using the Corel Photo-Paint software in order to get a neat contrast between the frozen and unfrozen areas. The resultant picture was then treated with the Global Lab Image software for calculating the average thickness of the frozen crust.

3. Modelling and simulation of the process

3.1. Mathematical model

In general, modelling of the freezing process is characterized by

Table 1
Characteristics of the products and their freezing conditions

Product	Geometry used for simulation	Average sizes (cm)	Average weight (g)	Immersion time (s)	Air-blast temperature ($^\circ\text{C}$)
Hamburger		$D = 10$ $L = 2$	150	20	-37
Meatball		$D = 5$	65	30	-38
Strawberry		$D = 3$ $L = 4$	10	20	-38

- (1) The existence of a region of discontinuity, which moves as a function of time in the boundary between the frozen and unfrozen phase.
- (2) The absorption or removal of an important amount of heat during the change of state.
- (3) A continuous modification of thermophysical properties of the product as a function of temperature.

In this case, modelling was carried out by means of a numerical method, which includes the change of phase phenomena in the thermal balance equations. So, the equations were solved in the whole system as if it were constituted by a single phase. Thus, the problem is transformed in a transient problem with temperature dependent properties.

The total process was considered as consisting of three successive stages:

1. Cryogenic freezing for $0 \leq t \leq t_1$.
2. Transport to the mechanical freezer for $t_1 < t \leq t_1 + t_2$.
3. Mechanical freezing for $t_1 + t_2 < t \leq t_1 + t_2 + t_3$ = freezing time.

For the three stages, the thermal balance to be solved is the same, but boundary conditions (ambient temperature T_∞ and heat transfer coefficient h) are different.

In this work, the numerical model was developed using the enthalpy method. For this purpose, the transient term of the thermal balance

$$\rho C_p \frac{\partial T}{\partial t} = \nabla(k \nabla T), \quad (1)$$

where ρ is the product density and k is its thermal conductivity, was expressed as

$$\rho \frac{\partial H}{\partial t} = \nabla(k \nabla T), \quad (2)$$

where H is the product enthalpy (J kg^{-1}).

This equation was solved with the enthalpy as the unknown variable on a fixed grid. Consequently, the knowledge of H allows to calculate the value of the temperature in each point of the grid. Then, the thermal conductivity and the position of the freezing front can be deduced. This formulation presents the advantage of being less sensible to the abrupt variation of the thermal properties within the phase change than the temperature formulation given by (1).

The thermal balance was solved using an explicit scheme for many regular geometric shapes, unidimensional (infinite cylinder, sphere, slab) and multidimensional (finite cylinder, disk, cone or a combination of them). The shapes used for the specific cases presented in this work are depicted in Table 1. The discretization of the equation was carried out by the finite volume method in such a way that thermal fluxes are conservative (Chau, Gaffney, & Romero, 1988; Tocci & Mascheroni, 1995).

The influence of grid size and spatial distribution was analyzed as regards to the predicted temperature profiles. The number of 31 gridpoints was established as adequate for obtaining a good precision. Their distribution along the main axis was done by dividing the region near the surface in equal volumes until reaching the one third of the radius, and the rest, in equal segments. The scheme of the discretization was chosen this way in order to get a narrower path in the outer part of the body, so that the frozen front advance during the immersion step can be accurately followed. Besides, the last gridpoint is near enough the geometric centre in order to take the temperature in this point as if it were the temperature of the centre, without major error.

The Fourier equation (2) takes the following form for an infinite cylinder:

$$\rho \frac{\partial H(T)}{\partial t} = \frac{1}{r} \frac{\partial}{\partial r} \left[k(T) r \frac{\partial T}{\partial r} \right] \quad (3)$$

and the initial condition is $T = T_0$ for $t = 0$. The boundary condition is

$$h(T_s)(T_\infty - T_s) = k(T) \left[\frac{\partial T}{\partial r} \right]_{r=R}, \quad (4)$$

where h is a function of the surface temperature T_s and R is the radius of the cylinder.

The discretisation for the interior gridpoints conducts to

$$\begin{aligned} \rho V_i \frac{H_i^{n+1} - H_i^n}{\Delta t} &= k_{i-1}^n A_{i-1} \frac{T_{i-1}^n - T_i^n}{r_{i-1} - r_i} - k_{i+1}^n A_{i+1} \\ &\quad \times \frac{T_i^n - T_{i+1}^n}{r_i - r_{i+1}}, \end{aligned} \quad (5)$$

where n is the time index; A_i the external surface of the volume element i ; i the space index ($i=0$ for the surface, $i=I$ for the centre, where I is the total number of points of the grid), and V_i is the volume between the gridpoints i and $i+1$.

For the centre point

$$\rho V_I \frac{H_I^{n+1} - H_I^n}{\Delta t} = k_I^n A_I \frac{T_{I-1}^n - T_I^n}{r_{I-1} - r_I}. \quad (6)$$

The enthalpy of external gridpoint is calculated from the general equation applying the boundary condition to a thin layer of the solid between the surface and the first point of the grid inside the body ($i=1$). The surface condition is thus expressed

$$h A_R (T_\infty - T_s) = k_1 A_1 \frac{(T_s^n - T_1^n)}{(R - r_1)}, \quad (7)$$

where A_R is evaluated at $r = R$.

3.2. Heat transfer coefficients and physical properties

In the case of the combined operation it must be taken into account that the heat transfer coefficient (h) changes under the operation time:

1. Until $t = t_1$, i.e., during the cryogenic stage, h is relatively high as regards the corresponding value for the mechanical stage (within $120\text{--}200 \text{ W m}^{-2} \text{ K}^{-1}$) (Macchi, 1995) and it also changes with time-on-stream because it depends on the surface temperature of the solid.
2. For $t_1 < t \leq t_1 + t_2$ and $t_1 + t_2 < t \leq t_1 + t_2 + t_3$, during the stages of transport in the air towards the mechanical freezer at room temperature and of freezing in the air-blast, respectively, h is much lower and constant in both cases (within $7 \text{ W m}^{-2} \text{ K}^{-1}$ and $30\text{--}45 \text{ W m}^{-2} \text{ K}^{-1}$, respectively).

The results of the simulation were compared in a first step to the experimental data obtained from Macchi (1995) for cylinders of gelatin with 70% of water. Gelatin was chosen as a model foodstuff in order to eliminate the heterogeneous characteristic of most foods. Nevertheless, it is representative from the thermal point of view of different kinds of food.

The functionality of H with temperature and other properties necessary for modelling the global process were also obtained from Macchi (1995). The enthalpy curve for gelatin presents a melting point of -13.9°C for a cooling rate of 0.1 K min^{-1} . The latent heat is 160 kJ kg^{-1} , the thermal conductivity is 0.55 W (mK)^{-1} and 0.95 W (mK)^{-1} for the fresh and frozen gel, respectively, and density is 1200 kg m^{-3} .

The heat transfer coefficient for the immersion step in LN is calculated from the following correlation for smooth cylinders in warming regime (Macchi, 1995):

$$h \text{ (W/m}^2\text{K)} = \frac{1860}{\Delta T_{\text{sat}}} + 125,$$

where $\Delta T_{\text{sat}} = T_{\infty} - T_s$. Besides, a value of $h = 7 \text{ W m}^{-2} \text{ K}^{-1}$ was taken for the transport in air stage and $h = 41 \text{ W m}^{-2} \text{ K}^{-1}$ during mechanical freezing.

In the case of hamburgers and meatballs, thermophysical properties were obtained from correlations found in the literature (Sanz, Domínguez, & Mascheroni, 1989) as a function of water content Y_o .

Melting point:

$$T_f = (1 - Y_o)/(0.06908 - 0.4393Y_o) \text{ (}^\circ\text{C)}.$$

Density

for $T \geq T_f$

$$\rho = 1053 \text{ (kg m}^{-3}\text{)}$$

for $T < T_f$

$$\rho = 1053/(0.98221 + 0.1131Y_o + 0.25746(1 - Y_o)/T) \text{ (kg m}^{-3}\text{)}.$$

Heat capacity

for $T \geq T_f$

$$C_p = 1448(1 - Y_o) + 4187Y_o \text{ (J kg}^{-1} \text{ }^\circ\text{C}^{-1}\text{)}$$

for $T < T_f$

$$C_p = 3874 - 2534Y_o + 902893(1 - Y_o)/T^2 \text{ (J kg}^{-1} \text{ }^\circ\text{C}^{-1}\text{)}.$$

Enthalpy

for $T \geq T_f$

$$H = 272637.584(1/T_{\text{ref}} - 1/T) + (1448(1 - Y_o) + 4187Y_o) \times (T - T_{\text{ref}}) \text{ (J kg}^{-1}\text{)}, T_{\text{ref}} = -40^\circ\text{C}$$

for $T < T_f$

$$H = (3874 - 2534Y_o)(T - T_{\text{ref}}) + 902893(1 - Y_o) \times (1/T_{\text{ref}} - 1/T) \text{ (J kg}^{-1}\text{)}.$$

Conductivity

for $T \geq T_f$

$$k = 0.0866 + 0.501Y_o + 5.05210^{-4}Y_oT \text{ (W m}^{-1} \text{ }^\circ\text{C}^{-1}\text{)}$$

for $T < T_f$

$$k = 0.378 + 1.376Y_o + 0.930/T \text{ (W m}^{-1} \text{ }^\circ\text{C}^{-1}\text{)}$$

In the case of strawberries, thermophysical properties were also obtained from correlations found in the literature. The calculated values for $Y_o = 0.91$ are the following:

Density (Miles, van Beek, & Veerkamp, 1983) for $T \geq T_f$ $\rho = 1035 \text{ kg m}^{-3}$, for $T < T_f$, $\rho = 957 \text{ kg m}^{-3}$.

Thermal conductivity (Succar & Hayakawa, 1983) for $T = -20^\circ\text{C}$, $k = 2.04 \text{ W m}^{-1} \text{ }^\circ\text{C}^{-1}$, for $T = 20^\circ\text{C}$, $k = 0.57 \text{ W m}^{-1} \text{ }^\circ\text{C}^{-1}$.

The enthalpy as a function of temperature was obtained from Dickerson (1981) and corrected for the initial water content according to the following data:

Initial phase change temperature (Tocci, Spiazzi, & Mascheroni, 1998): $T_f = -1^\circ\text{C}$.

Enthalpy of melting (Tocci, Spiazzi, & Mascheroni, 1998), $\Delta H_m = 305000 \text{ J kg}^{-1}$.

Phase change temperature range (Tocci, Spiazzi, & Mascheroni, 1998) $\Delta T_f = 8^\circ\text{C}$.

The values of the curve taken for the enthalpy function are consistent with other results for strawberries found in the literature such as:

Heat capacity (Delgado, Rubiolo, & Gribaudo, 1990): for $T = 20^\circ\text{C}$ $C_p = 3759 \text{ J kg}^{-1} \text{ }^\circ\text{C}^{-1}$, for $T = -20^\circ\text{C}$, $C_p = 2325 \text{ J kg}^{-1} \text{ }^\circ\text{C}^{-1}$.

During modelling for the cryomechanical freezing of gelatin cylinders it was noticed that, actually, the value of h changes very little during the immersion stage in

liquid N₂ (within $3 \text{ W m}^{-2} \text{ K}^{-1}$). This is particularly true if immersion time is as short as it is normally for a cryomechanical process. Thus, in the case of cryomechanical freezing of hamburgers, meatballs and strawberries a constant value of h was used for the immersion step, independently of the surface temperature. These values were $h = 170, 235$ and $190 \text{ W m}^{-2} \text{ K}^{-1}$ for hamburgers, meatballs and strawberries, respectively. They were experimentally obtained for typical immersion time and therefore, they represent average values. They are in the range of other values found in the literature for immersion in LN (Cowley, Timson, & Sawdye, 1962; Merte & Clark, 1964; Bergles & Thompson, 1970). Besides, $h = 7 \text{ W m}^{-2} \text{ K}^{-1}$ was taken for the transport in the air step and, $h = 34, 40$ and $42 \text{ W m}^{-2} \text{ K}^{-1}$ for hamburgers, meatballs and strawberries, respectively, for the mechanical freezing stage.

4. Results and discussion

4.1. Model food

4.1.1. Cylinders of gelatin. Validation of the model

Calculated and experimental temperature profiles obtained during the freezing of the gelatin cylinders in the cryomechanical freezer for an immersion time in LN of $t_1 = 30 \text{ s}$, a transport time in the air of $t_2 = 0 \text{ s}$, and an air-blast temperature of -40°C are shown in Fig. 1. The correspondents to mechanical freezing only, i.e., for $t_1 = 0 \text{ s}$, are presented in Fig. 2. These profiles belong to different positions along the radius of the cylinder. Even the abrupt freezing of the most external layers of the body due to immersion in LN can be accurately fol-

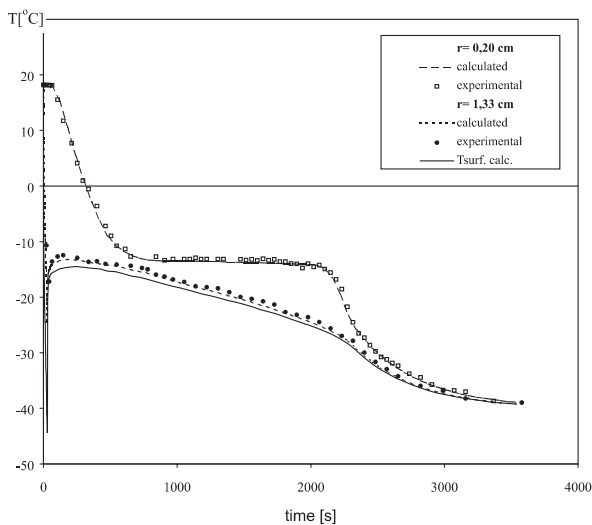


Fig. 1. Experimental (Macchi, 1995) and calculated temperature profiles for gelatin cylinders ($D = 3 \text{ cm}$, $L = 10 \text{ cm}$) at different radius, frozen in the cryomechanical freezer ($T_{\text{air}} = -40^\circ\text{C}$, $t_1 = 20 \text{ s}$, $t_2 = 0 \text{ s}$).

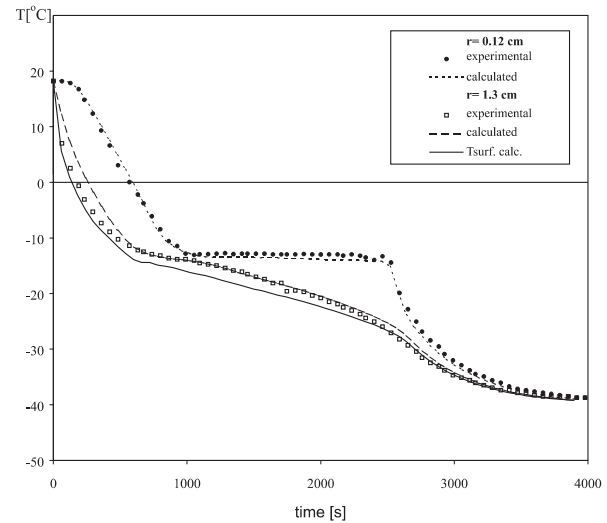


Fig. 2. Experimental (Macchi, 1995) and calculated temperature profiles for gelatin cylinders ($D = 3 \text{ cm}$, $L = 10 \text{ cm}$) at different radius, frozen in the mechanical freezer ($T_{\text{air}} = -40^\circ\text{C}$).

lowed (for example, for $r = 1.33 \text{ cm}$ in Fig. 1). It can be noted that the calculated profiles are very close to the experimental thermal history of the model foodstuff. So, despite its simplicity, the proposed model represents satisfactorily the thermal process.

In order to predict the effect of two of the main variables of the cryomechanical process, the model was run for different values of t_1 and t_2 , i.e., the immersion time and the time of transport in the air at room temperature, respectively. Figs. 3 and 4 show the calculated temperature profiles for the centre of the body, in each case.

It can be remarked that the total freezing time is reduced when the immersion time is increased (Fig. 3).

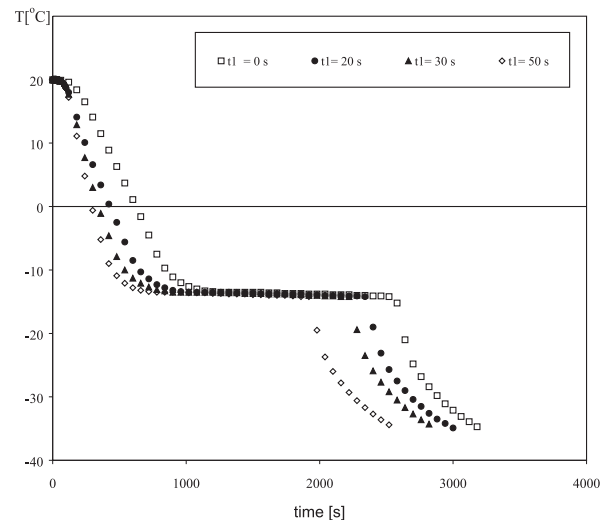


Fig. 3. Effect of the immersion time in LN t_1 on the temperature profile calculated for the centre of the cylinder of gelatin with $t_2 = 0 \text{ s}$.

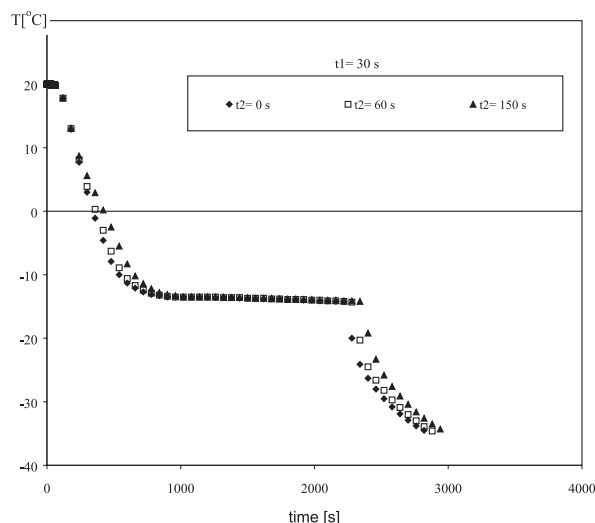


Fig. 4. Effect of the transport time in the air t_2 on the temperature profile calculated for the centre of the cylinder of gelatin with $t_1 = 30$ s.

This is a clear consequence of the low temperature and the high heat transfer coefficient inherent to the cryogenic stage. For an immersion time $t_1 = 50$ s, the total freezing time is reduced by 20% as regards mechanical freezing. On the contrary, the transport time t_2 is not relevant for the total freezing time (Fig. 4). For $t_1 = 30$ s, a transport time $t_2 = 150$ s generates an increase of 5% in the total freezing time in relation to the value for $t_2 = 0$ s.

Experimental and calculated values of the crust thickness are presented in Table 2. As shown, the simulation of the cryomechanical process allows satisfactorily to predict the depth of the crusted layer.

The predicted influence of t_1 and t_2 on the crust thickness is presented in Fig. 5. As shown in the figure, the cryomechanical freezing provokes a quick freezing of the outer surface layer (crust), which makes the product more resistant from a mechanical point of view. In fact, in absence of the cryogenic stage, the surface freezing hardly begins after 9 min meanwhile crust formation takes only a few seconds in the combined freezer. However, the immersion time must be prolonged in the case that the transfer time in air is increased.

Table 2
Comparison between calculated and experimental frozen crust thickness (from Macchi, 1995) as a function of immersion time in LN

Immersion time (s)	Calculated thickness (cm)	Measured thickness (cm)
10	0.05	0.03
15	0.08	0.08
20	0.11	0.11
25	0.15	0.14
30	0.16	0.17

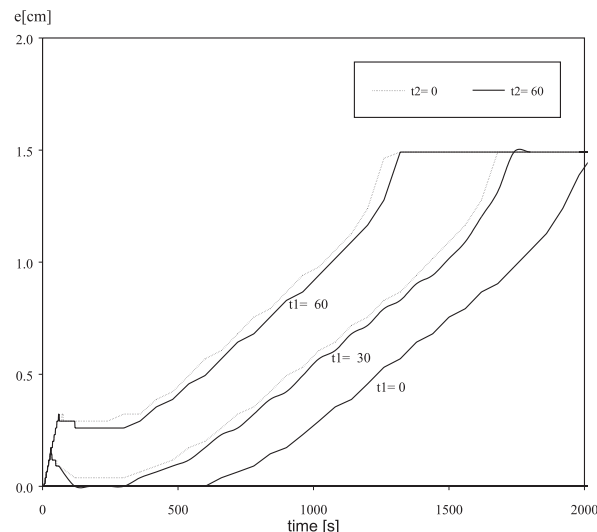


Fig. 5. Calculated width (e) of the crust formed during cryomechanical freezing. Effect of the immersion time in LN t_1 and the transport time in the air t_2 .

4.2. Real food

4.2.1. Hamburgers and meatballs

Fig. 6 presents the experimental and calculated results during hamburger freezing in the combined freezer and in the mechanical one. As it can be seen, the agreement between the experimental and calculated data is quite good, taking into account the experimental error and the approximations in coefficient and property values introduced in the model. A similar behavior can be observed in the case of meatballs (Fig. 7).

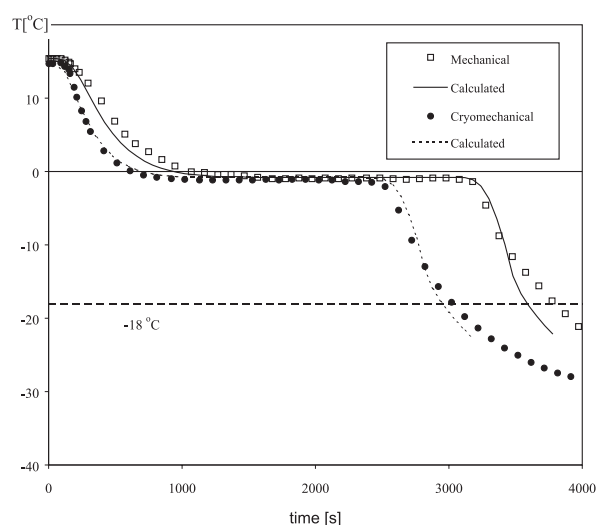


Fig. 6. Experimental and calculated temperature profiles evaluated at the centre for hamburgers ($D = 10$ cm, $L = 2$ cm) frozen in the cryomechanical ($T_{\text{air}} = -40^\circ\text{C}$, $t_1 = 20$ s, $t_2 = 0$ s) and the mechanical freezer ($T_{\text{air}} = -40^\circ\text{C}$).

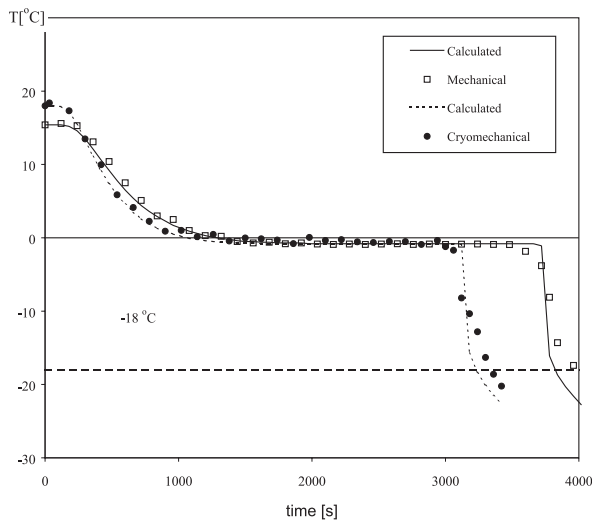


Fig. 7. Experimental and calculated temperature profiles evaluated at the centre for meatballs ($D=5$ cm) frozen in the cryomechanical ($T_{\text{air}}=-40^{\circ}\text{C}$, $t_1=30$ s, $t_2=0$ s) and the mechanical freezer ($T_{\text{air}}=-40^{\circ}\text{C}$).

4.2.2. Strawberries

Temperature profiles during freezing for strawberries are presented in Fig. 8. Obviously, in this case the calculated curves are not as accurate as for meatballs and hamburgers. This result can be ascribed to the fact that a cone shape is a rough simplification of the geometry of a strawberry. Another possible source of error can be attributed to less precise k – T and/or H – T relationships at low temperatures than for the upper temperature range, leading to a distorted temperature profile. In spite of this fact, it can be inferred that the model represents the process of heat transfer in a real foodstuff with a high

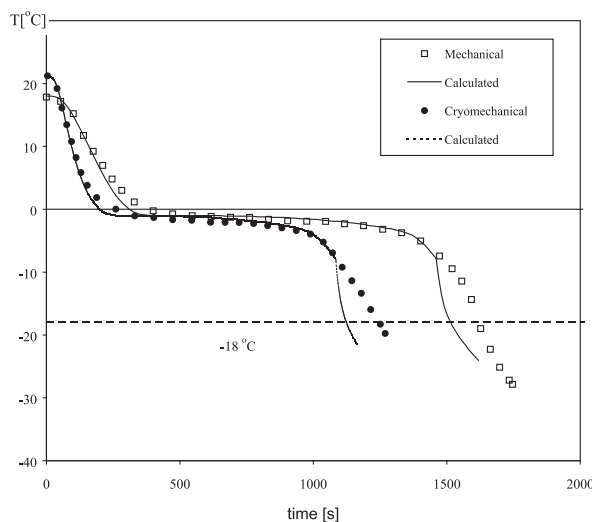


Fig. 8. Experimental and calculated temperature profiles evaluated at the centre for strawberries frozen in the cryomechanical ($T_{\text{air}}=-40^{\circ}\text{C}$, $t_1=20$ s, $t_2=0$ s) and the mechanical freezer ($T_{\text{air}}=-40^{\circ}\text{C}$).

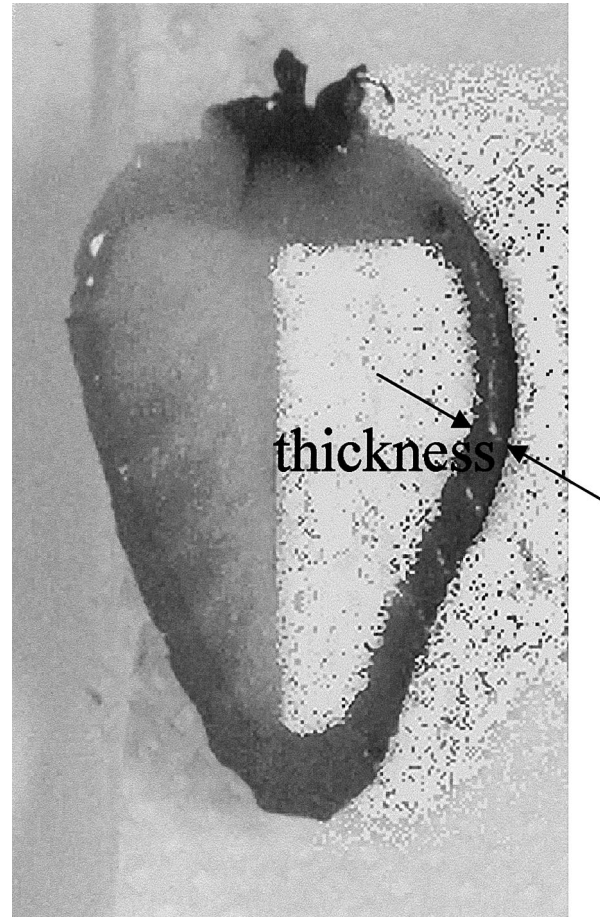


Fig. 9. Worked out photograph of half a strawberry showing the depth of the crust-frozen zone.

degree of accuracy. The goodness of model application was also tested for the prediction of the thickness of the frozen crust of strawberries during immersion in LN. In this case, the crust thickness could be easily measured from photographs and image analysis as described above. Fig. 9 shows a photograph of a strawberry submerged in LN for 15 s, which has been partially worked out to better depict the procedure for thickness evaluation. The measured values as a function of the immersion time are presented in Table 3. As it can be observed, the calculated values are in very good agreement with the measured ones.

Table 3

Comparison between calculated and experimental frozen crust thickness for strawberries as a function of immersion time in LN

Immersion time (s)	Calculated thickness (cm)	Measured thickness (cm)
5	0.020	0.03
10	0.65	0.6
15	0.115	0.10
20	0.165	0.15

5. Conclusions

The simulation of the cryomechanical process presented in this work was successfully validated with experimental results obtained from the literature for a model food (gelatin) and our own data for real foods.

The model allows us to predict the temperature profile within the food, the freezing time and the thickness of the frozen crust. Obviously, the fit is better for real foods with regular geometrical shapes as in the case of hamburgers and meatballs, than for foods presenting irregular forms as in the case of strawberries. Nevertheless, the model is enough good to get a good approximation for the values of the freezing time and of the thickness of the crust. This last parameter is particularly important to optimize the cryomechanical process. Actually, this value can be related to the gain in mechanical resistance as a function of immersion time for determining the minimum proportion of the cryogenic step.

References

- Acharya, A., Marchese, M. A., Bredencamp, D. (1989). Cryomechanical freezing of strawberries. *IIR Commissions C2, D1, D2/3, Davis, CA*, pp. 277–281.
- Bergles, A. E., & Thompson, W. G. (1970). The relationship of quench data of steady-state pool boiling data. *International Journal of Heat and Mass Transfer*, 13, 55–68.
- Chau, K. V., Gaffney, J. J., & Romero, R. A. (1988). A finite difference model for heat and mass transfer in products with internal heat generation and transpiration. *Journal of Food Science*, 30, 484–487.
- Cowley, C. W., Timson, W. J., & Sawdye, J. A. (1962). A method for improving heat transfer to a cryogenic fluid. *Advances in Cryogenics Engineering*, 7, 385–390.
- Delgado, A. E., Rubiolo, A. C., & Gribaudo, L. M. (1990). Effective heat capacity for strawberry freezing and thawing calculations. *Journal of Food Engineering*, 12, 165–175.
- Dickerson, R. W. (1981). Enthalpy, specific heat and thermal diffusivity of frozen foods. In: *Handbook of product directory fundamentals* (pp. 9–11, Chapter 30). New York: American Society of Heating, Refrigeration and Air Conditioning Engineers.
- Groll, M. (1986). Les nouveaux systèmes de surgélation cryogénique, *RGF*, September, pp. 448–450.
- Gruda, Z. (1999). The combined fluidized bed and LN₂ freezing. In *Proceedings of the 20th International Congress of Refrigeration*. Sydney, Australia (in press).
- Londhal, G., Goranson, S. (1995). Quality differences in fast freezing. In *Proceedings of the 19th International Congress of Refrigeration* (vol. I, pp. 197–203).
- Macchi, H. (1995). Congélation alimentaire par froid mixte: Procédé avec prétraitement par Immersion dans l'Azote Liquide. *Doctoral Thesis, ENGREF* (pp. 248), Paris, France.
- Merte, H., & Clark, J. A. (1964). Boiling heat transfer with cryogenic fluids at standard, fractional and near zero gravity. *Journal of Heat Transfer*, 86, 351–359.
- Miles, C. A., van Beek, G., Veerkamp, C. H. (1983). Calculation of thermophysical properties of foods. *Physical Properties of Foods Applied Science* (pp. 269–312, Chapter 16), London.
- Sanz, P. D., Domínguez, M., & Mascheroni, R. H. (1989). Equations for the prediction of thermophysical properties of meat products. *Latin Am. Appl. Res*, 19, 155–164.
- Succar, J., & Hayakawa, K. (1983). Empirical formulae for predicting thermal physical properties of food at freezing or defrosting temperatures. *Food Science Technology*, 16, 326–331.
- Summers, J. (1986). Cryogenic food freezing in today's market and its costs related to conventional mechanical systems. *AICHE Symposium Series No 84*, pp. 241–249.
- Tocci, A. M., & Mascheroni, R. H. (1995). Numerical models for the simulation of the simultaneous heat and mass transfer during food freezing and storage. *International Communication on Heat and Mass Transfer*, 22(2), 251–260.
- Tocci, A. M., Spiazzi, E. A., & Mascheroni, R. H. (1998). Determination of specific heat and enthalpy of melting by DSC. Application to osmo-dehydrated fruits. *High Pressures-High Temperatures*, 30, 357–363.